Imperial College London

harefield heartsciencecentre

Characterisation of Myocardial Slices for Physiological and Pharmacological Studies

Sara Mamdouh Abou Al-Saud

Academic Supervisor

Dr.Cesare Terracciano

Imperial College London

Co-Supervisor

Dr.Patrizia Camelliti

Oxford University

5280 Words

MRes in Biomedical Research

12th March 2010

Acknowledgements

I would like to thank my supervisor, Dr Cesare Terracciano for his support and guidance in this work. He has been a source of great inspiration whilst showing endless patience and I am very grateful. I would like to thank my co-supervisor, Dr Patrizia Camelliti for her continuous support, tenderness, and encouregment especially by allowing me to use her novel develped protocol for obtaining intact myocardial tissue slices. Many thanks to Toxicology Control Animals – Pfizer for supplying the dog myocardial tissue. I am grateful to my friends from Cell Electrophysiology who were always encouraging me and making time in the lab so enjoyable; in particular Dr Urszula Siedlecka for perpetual support in the lab, and my colleague (PhD student) Michael Ibrahim who continually encouraged me and was a constant source of lively discussion. Not to forget Dr Manoraj Navaratnarajah for his help arranging the human tissue biopsies collection at Harefield Hospital, Dr Aalya Malik, Dr Padmini Sarathchandra, and Dr Ryszard Smolenski.

I thank King Saud University, King Fahad Cardiac Centre and The Magdi Yacoub Institute for financial support during my study. I express my gratitude to my family who supported me throughout my time of study, particularly my mother and father who gave so much without limitations, my brother who was always there for me, and my lovely little sister who is always a listener, counsellor , supporter , lover, helper and a sharer of delights. And last but not least, my dearest friend (PhD student) Samha Al-Ayoubi, there is no better friend than a sister and there is no better sister than her.

To Hanaa Al-Kilani & Mamdouh Abou Al-Saud……

Table of contents

List of Figures & Tables

Figures No.

Table No.

Abbreviations

AP	-	Action Potential
APD_{90}	-	Action Potential Duration at 90% Repolarisation
CV	-	Conduction Velocity
DCM	-	Dilated Cardiomyopathy
FP	-	Field Potential
FPD	-	Field Potential Duration
HCM	-	Hypertrophic Cardiomyopathy
I_{Kr}	-	Rapid Delayed Rectifier Potassium Current
I_{Ks}	-	Slow Delayed Rectifier Potassium Current
LVAD	-	Left Ventricular Assist Device
MEA	-	Multi-electrode Array
NT	-	Normal Tyrode
SR	-	Sarcoplasmic Reticulum

ABSTRACT

Aim: Enzymatically digested cardiomyocytes have been used extensively to study cardiac function. The multicellular level is less characterised. The aim of this study was to validate a novel slicing technique to obtain multicellular preparations using adult rat, dog, and human cardiac tissue. We investigated whether heart slices could be used as a model to understand cardiac function; specifically, we studied electrical stimulation, conduction, and propagation, thereby, giving insight into cell-to-cell interaction. **Methods:** Vibrotome cut myocardial ventricular slices (350 μm thick) were obtained from rat, dog, and human; all were electrophysiologically assessed. Field potential duration (FPD) was recorded using multi-electrode arrays (MEAs). Different drugs (E-4031 and Chromanol 293B) were used to assess the response to pharmacological challenge. Homogeneity of tissue slices was tested measuring local and peripheral conduction velocities (CV). Anisotropic properties of cardiac tissue were also investigated. **Results:** The response of the slices to the two well known potassium channel blockers E4031 and Chromanol 293B, produced a prolongation of FPD in myocardial tissue slices. E-4031 (1 μM) prolonged FPD in dog ventricular slices by 18%, human dilated cardiomyopathy (DCM) ventricular slices by 32%, and myocarditis ventricular slices by 29%. Chromanol 293B (20μM) had a smaller effect on dog ventricular slices prolonging FPD by approximately 10%. Analysis of the spread of excitation shows that CV in the direction of cardiac fibres is 2 - 3 times faster than in the perpendicular direction, supporting the anisotropic properties of cardiac slices. **Conclusion:** Viable ventricular slices are a representative tool for studying the electrophysiological and pharmacological properties of the myocardium at the multicellular level.

1. INTRODUCTION

1.1 Normal Cardiac Properties

1.1.1 Conduction System

The contraction of the heart is regulated by many systems within and external to the heart. The cardiac conduction system is responsible for the co-ordination of cardiac contraction by converting an electrical signal into mechanical activation. It consists of the sinoatrial node (SA node), atrioventricular node (AV node), Bundle of His, Bundle branches and Purkinje fibers (1). The pacemaker in the heart, consisting of specially modified cells, is the source of the electrical firing that leads to the generation of cardiac action potential (AP) (2).

1.1.2 AP

AP is the transient voltage alteration across the cardiomyocytes membrane (3). Current formation is due to the inward and outward movement of ions through ion channels in the lipid bilayer of the cells membrane (4). AP starts when the SA node fires, an electrical excitation of the cell surface membrane (sarcolemma) produces a wave of depolarisation due to the influx of Na^+ and Ca^{2+} (3). The voltage gated Na^+ channel opening generates an inward current responsible for the upstroke of the AP. The voltage gated K^+ channels open due to the increment of the positive charges inside the cell and potassium outward current takes place (Figure 1).

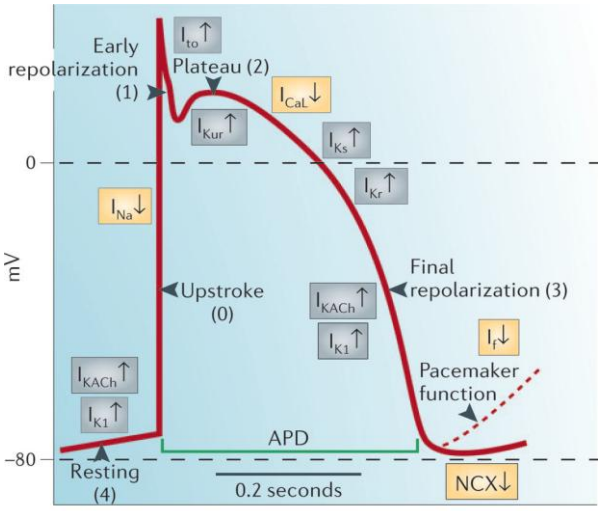

Figure 1: Normal cardiac AP showing all phases involved. Resting membrane potential (4), Depolarisation / stimulation and raising due to Na^+ influx (0), Early polarisation / peak due to K^+ efflux (1), Plateau / falling due to Ca^{2+} influx(2), Final repolarisation/ hyperpolarisation due to outward K^+ flow(3) phases. (5)

Ca^{2+} flows into the cell through the L-type Ca^{2+} channel and induces the release of Ca^{2+} from sarcoplasmic reticulum (SR) through the ryanodine receptor (RyR) (3).

1.1.2.1 Contraction

The mechanical effect takes place when the Ca^{2+} released from SR binds to the troponin-tropomyosin complex. This binding shifts the troponin exposing the actin binding sites to the myosin heads hence producing muscle contraction (3).

1.1.2.2 Relaxation

Relaxation is essential for normal cardiac function. Relaxation involves the rapid removal of Ca^{2+} from the cytosol. This removal is achieved through Ca^{2+} extrusion mechanisms: firstly the SR Ca^{2+} -ATPase (SERCA2a) removes Ca^{2+} from the cytosol into the SR. Secondly the Na^{+}/Ca^{2+} exchanger (NCX) removes Ca^{2+} from the cell into extracellular space whilst bringing Na^{+} into the cell. Outward potassium ion channels open, efflux of potassium ions lead to decrease in the positivity of the membrane potential. This fluctuation of ions results in repolarisation of the cell membrane allowing for the next wave of depolarisation and hence rhythmic contraction (3).

1.1.3 Cardiac Ion Channels

AP is generated due to the complex interplay of cardiac ion channels. Ion channels have two primary properties, ion permeability and gating. Selective permeability of ion channels describes the movement of specific ions through specific ion channels such as Na^{+}, K^{+} and Ca^{2+} channels. Gating, which is the property of the opening and closing of ion channels, has three mechanisms' voltage dependent, ligand-dependent and mechano-sensitive gating. Voltage gated channels conductance depends on the variations of membrane potential and majority of these channels open in response to depolarization (5).

1.1.3.1 Cardiac Potassium Ion Channels

Cardiac potassium ion channels are responsible for repolarising excited cells and reaching the resting membrane potential (6). According to the mode of activation, potassium ion channels have been classified into four structural types. Inward rectifier potassium channels - K_{ir} , Ca^{2+} - activated potassium channels - K_{Ca}, background leak potassium current - K_{2P}, and Voltage gated potassium channels - K_V (I_{to}, I_{Kur}, I_{Kr}, I_{Ks})(7-9).

1.1.3.2 Voltage Gated Potassium Channels

Voltage Gated Potassium Channels are composed of 4 α-subunit and multiple ß-subunits. Each α-subunit contains six transmembrane segments (S1-S6). Segment four (S4) acts as a voltage sensor domain. α-subunit major subfamilies include the hERG channel (gene KCNH2) responsible for I_{Kr} - rapid delayed rectifier potassium current, and K_VLQT1 (gene KCNQ1) responsible for I_{KS} - slow delayed rectifier potassium current. They are in charge of generating the outward delayed rectifier potassium current in the heart for controlling action potential repolarisation, and therefore cardiac action potential duration (APD_{90}) (9;10).

1.1.3.3 Voltage Gated Potassium Channels as a Therapeutic Targets

Voltage gated potassium channel function can be either affected by altering the channel gating by partial or complete binding to the voltage sensor domain or by blocking the ion conducting pore from either sides internally or externally (9). Class III anti-arrhythmic drugs, such as E-4031 (I_{Kr} channel blocker) (11) and Chromanol 293B (I_{Ks} channel blocker)(12;13), have been previously used to test the properties of these channels. These agents have greatly lengthened APD_{90} in different cardiac research models (14-17).

1.1.4 Gap Junction Channels

The wave of depolarisation travels from one myocyte to another via gap junctions (18). The major cardiac gap junction and principle intercellular coupling protein is connexin 43 (Cx43) (19). The main role of gap junctions is forming low resistance connections between myocytes (5). Impulse propagation between cells depends on gap junction distribution. Gap junctions' disorganisation and pathological remodelling has been shown to contribute to arrhythmogenesis (20;21).

1.1.5 Anisotropic Conduction Properties

The direction in which cardiac fibres are oriented, affects the propagation and specifically CV of the electrical stimulus, which is the excitation speed from one myocyte to another (22;23). Cardiac anisotropism determinants are cell architecture, size, directional distribution of gap junctions, and age of the individual (23;24). Cellular coupling resistance is affected by the heart anatomical anisotropic variations (22;23). Less resistance occurs parallel to the longitudinal axes of the fibres due to gap junction than perpendicular to them. Any changes in fibre direction appear to play an important role in wave discontinuously leading to arrhythmogenesis (23).

1.2 Cardiac Diseases

1.2.1 Cardiomyopathies

Cardiomyopathies are diseases characterized by degeneration of cardiac muscle (25). They are divided into primary and secondary cardiomyopathies (25). Primary cardiomyopathies include *dilated cardiomyopathy* (DCM) and *hypertrophic cardiomyopathy* (HCM). DCM is the weakness of cardiac muscle associated with chamber enlargement and muscle thinning affecting its ability to pump blood (26), whereas HCM is referred to hypertrophied myocardium associated with sudden cardiac death (27). One main cause of secondary cardiomyopathies is cardiac muscle inflammation referred as *myocarditis* (25). *Myocarditis* is mainly due to viral infections (28). The best treatment option for end stage cardiomyopathy patients is heart transplantation. Due to the small number of hearts donors, *ventricular assist devices* (VADS) are used (29). VADS are used predominantly to keep patients alive while waiting for transplantation.

1.2.2 Arrhythmias

Once SA node fires, AP propagates to AV node. The propagation continues to Bundle at a slower velocity, to ensure that the atrial contraction precedes the ventricular contraction (30). The Purkinje system distributes the electrical stimulus to the ventricular myocardium resulting in synchronized

ventricular contraction. Disturbance or malfunction of any of part of the conduction system due to heredity, stress, drugs, etc is highly life threatening as it may lead to cardiac arrhythmias (1).

1.3 Cardiac Research Models

Electrical activity of the heart is fundamental to its contractile function. This activity is due to cellular processes, and to multicellular interaction. Several model systems have been used for studying cardiac function including the whole heart, tissue segments such as papillary muscle or coronary-perfused wedges and cardiomyocytes either isolated or cultured, but there is debate on which of these models is most representative of whole heart function *in vivo (31).*

Cardiac tissue slices may offer a realistic *in vivo* model of myocardium, suitable for a wide range of investigations, as they potentially retain the relevant structural and functional characteristics of native tissue. The slicing technique has been used previously to obtain ventricular slices from neonatal murine (32) and adult mouse (33). To overcome some of the technical issues such as oxygen diffusion limitations resulted from embedding the ventricle into 4% low-melt agarose and long handling time, a new method was developed by Bussek et al. (34) which benefits from less invasive procedure.

Table 1: Comparison between different models to study cardiac function:

Advantages	talosIed setycoym model	Multicellular model "Cultured"	Multicellular model "Tissue slice"	traeh elohW model
Myocytes distribution	X	√ Non realistic	√ realistic	√ realistic
Intact multicellular structure	X	√ Non realistic	√ realistic	√ realistic
Cell-to-cell interaction	X	√ Non-realistic	√ realistic	√ realistic
Intercellular communication	X	√	√	√
Homogeneity	X	√	√	√
Ease of preparation	X	X	√	X
Oxygen diffusion	√	√	√	√
Real microenvironment	X	X	√ Mini-model	X
Enzymatic digestion	√	√	X	X
Model popularity in cardiac research	√	√	X	√
Number of results obtained / heart	high	low	high	low

1.3.1 Previous Studies Using Cardiac Slices

In 1976, cardiac slices were first used for molecular investigations by Claycomb *et al*. – for a review see (35). Afterwards, in the 1980's, cardiac slices attracted researchers in different fields. Pharmacological studies were applied to assess the toxicity effect of several substances such as mitoxantrone by measuring the oxygen uptake and ATP production in slices (36). Soon after, application of the cardiac slice model to metabolism research was investigated measuring the O_2 consumption of normal and pathologically disturbed myocardium (37). Electrophysiological properties were tested using patch-clamp techniques , similar to brain slice experiments (38).

Here, I have used a method developed by Camelliti et al. (39), to prepare and maintain living cardiac ventricular slices obtained from adult rat and dog hearts, and from human ventricular biopsies obtained from patients undergoing heart transplants or LVAD implantation.

1.5 Hypotheses

The main hypothesis of this project is that cardiac slices are a reliable and reproducible model to study the functional properties of the myocardium. The aims of this study are to investigate the following:

1) To determine whether myocardial slices are viable for electrophysiological recordings using MEAs.
2) To assess whether the electrical recordings observed from these slices mimic physiological readings.
3) To study whether there are species differences in electrophysiological parameters using slices preparations.
4) To determine if the specific ion channel blocker E-4031 and Chromanol 293B affects repolarisation in myocardial slices.
5) To study the conduction velocity of the slice preparations.
6) To study the anisotropism of the slice preparations.

Different species with normal and abnormal myocardial tissue were used to address there hypotheses. Rat, dog and human cardiac tissue were assessed.

2. MATERIALS & METHODS

2.1 Preparation of Slices

Cardiac left ventricular myocardial slices were obtained from different species including rat, dog, and human. Rat cardiac tissue obtained from Lewis rats aged 12-16 weeks (Charles River) was preserved in Normal Tyrode (NT) (in mM: 140 NaCl, 6 KCl, 10 glucose, 10 HEPES (free acid), 1 MgCl2, 1 CaCl2; pH 7.4; chemicals purchased from VWR, England) + heparin (10units/ml, purchased from LEO-Laboratories Limited, UK). Dog cardiac tissue was obtained from Beagle dogs aged 12-18 months (Toxicology control animals - Pfizer, Sandwich, Kent, UK) preserved in cardioplegia solution (CP) (containing in 20ml: Magnesium Chloride BP3.253g, Potassium Chloride BP 1.193g, Procaine Hydrochloride BP 272.8mg; purchased from Martindale Pharmaceuticals, UK) at 4°C. Human ventricular seispoib in this study were obtained from three cardiomyopathy patients: (1) from heart transplant for DCM patient, (2) from LVAD implantation to myocarditis patient, and (3) from myectomy to HCM patient. All human cardiac biopsies were preserved in cold CP.

All animal procedures were performed according to UK Home Office Regulations and passed ethical review. Patients provided consent for the use of their tissue for research and this process passed local ethical review by the Royal Brompton, Harefiled and NHLI Research Ethics Committee.

A cube of left ventricular myocardial tissue (0.7cm^3) was cut and glued - using surgical tissue adhesive (3M-Vetbond, No.1469SB) - to a 4% agarose block. The agarose block was fixed by super glue to the metal cutting stage of the high precision vibrotome (7000 smz, Campden Instruments Ltd., UK), in order to obtain viable myocardial slices. Horizontal cutting direction was used in order to obtain maximum number of living cells organised in the same fibre direction.

The vibrotome was set to cut slices at 350µm thickness, with extremely low cutting speeds (0.03mm/s), high amplitude and frequency (2mm; 75Hz), and submicron blade Z deflection (essential

for reproducible generation of viable cardiac slices). Stainless steel blades were used for cutting (Campden Instruments limited, No.7550/1/SS).

The cutting process was carried out in a cold (4°C) oxygenated NT solution (Ca^{2+} 1.8 mM) containing a contraction uncoupling agent, 2,3-butanedione monoxime (BDM,10mM), (Sigma Aldrich, Deisenhofen, Germany). Slices were transferred from the bath of the vibrotome to a baker containing oxygenated NT-BDM solution at room temperature. The slices were placed on a nylon mesh surface to ensure fully oxygen diffusion to the inferior surface. In order to prevent the samples from curling up, slice holders were used. These are metal rings (A4 from Washers, No.51875) covered by fine mesh (Cadisch precision meshes ltd, No.0614).

2.2 MEA

In order to measure the sequential excitation of cardiac myocytes within each slice, an MEA with 60 silicone – polyimide microelectrodes , arranged in an 8 X 8 layout grid and interelectrode distance of 700µm (Multichannel systems, MEA1060, No.0133), was used . The MEA was connected to an amplifier system (Multi Channel System, Reutlingen, Germany), which included a heating system. Tissue slices were transferred from the NT-BDM container to the MEA and electrical responses were recorded from different electrodes for electrophysiological assessment.

2.3 Field Potentials (FP) Recordings

Superfusion chamber. Myocardial slices were placed in MEA dish and continuously superfused with oxygenated NT solution at 37°C. Electrical unipolar stimulation was applied starting with pulses of 1V and duration of 500 µs, at a frequency of 1Hz for 10 minutes. Voltage amplitude and duration were increased up to 8V and 2ms depending on the slice response.

Superfusion was controlled manually using a 4-channel valve system. FPD was recorded at different stages. Control recordings were taken after 10 minutes of NT perfusion. Addition of the drugs E-4031(1µM - Tocris, No.1808) or Chromanol 293B (20µM - SIGMA, No.C2615) took place and

subsequently recordings were taken after 2, 5, 10 and 15 minutes of superfusion (each recording lasts for 20 seconds) followed by 10 minutes wash out. Data acquisition and electrical stimulation were controlled via an automated software programme (Multi Channel Systems, MC_Rack). The resulting data were analysed using Clampfit 10.0 (Axon CNS Molecular devices) and Excel (Microsoft).

2.4 CV Recordings

Cardiac slices were superfused by oxygenated NT at 37°C, unipolar stimulation was applied from different electrodes to measure different CVs correlated to slice fibres directions. The traces were recorded using the software MC_Rack (Multichannel systems). This experiment lasted 5-10 minutes for each slice. The data obtained were analysed using MATLAB (The Mathworks, Natick, USA), MEA Tools Software and Excel (Microsoft).

CVs were also recorded from cardiac slices superfused with KREBS solution (in mM: NaCl 120; KCl 4.7; $MgSO_4 \cdot 7H2O$ 0.94; KH_2PO_4 1.22; $NaHCO_3$ 25, glucose 11.54; PH 7.4. (Chemicals were purchased from VWR, England).

2.5 Statistical Analysis

Data are expressed as mean ± SEM, and analyzed using one-way ANOVA followed by post Tukey test or Unpaired Student's t-Test. All statistical analysis and graphs were performed using Prism 4 programme (GraphPad Software, Inc. USA). *P values* < 0.05 (95% confidence level) were considered significant.

3. RESULTS

3.1 Slices Preparation Efficiency

The quantity of cardiac slices obtained depends on ventricular wall thickness which varies according to the species. From rat ventricular myocardial tissue approximately 7 slices per heart could be obtained, whereas more slices could be obtained from dog ventricular myocardial tissue (approximately 15 slices per heart). The numbers of slices obtained from human biopsies varies according to the thickness of the biopsy, but approximately 6 slices per heart could be cut. Stable electrophysiological properties could be seen in 90% of the slices.

3.2 Electrophysiological Measurements

3.2.1 AP Measurements

To measure AP, different experimental methods have been used such the patch clamping technique. They were used for measuring AP from one excited cell or cells in the whole tissue to study cell-to-cell interactions.

3.2.2 FP as an AP Surrogate

Extracellular FP is the measurements of voltage produced outside the cells during stimulation. To correlate AP and FP measurements, the upstroke of AP (phase 0) was correlated to the down stroke in FP (Figure 2, (40)). APD measured from the point of the upstroke to the time of 90% repolarisation APD_{90} was similar to the FPD measured in the same way. A linear relationship was observed between APD_{90} and FPD supporting the hypothesis that FP can be used as an AP surrogate (41).

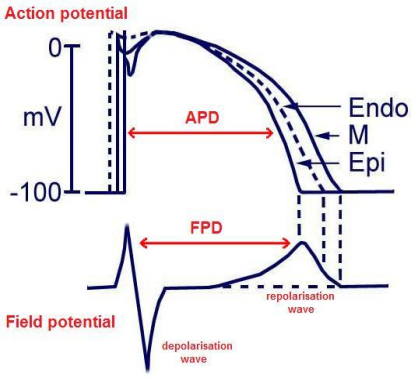

Figure 2: Correlation between APD and FPD measured from the same cell. (40) modified.

3.2.3 FP Recordings

The effects of drugs on cardiac slice repolarisation were assessed by measuring FPD before and after the addition of 1µM E-4031 or 20µM Chromanol 293B. Two waveforms can be detected in the FP. One fast large depolarisation wave and other slower smaller repolarisation wave. The repolarisation wave is clearly detected in dog and human ventricular myocardial slices, whereas it is less evident in rat ventricular myocardial slices (Figure 3).

A.

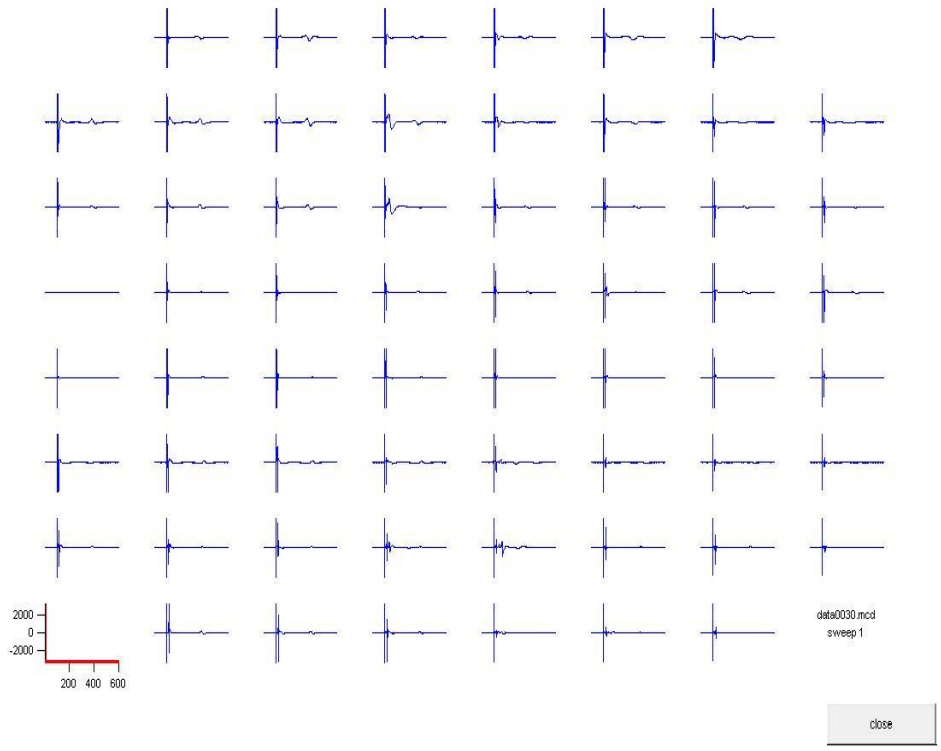

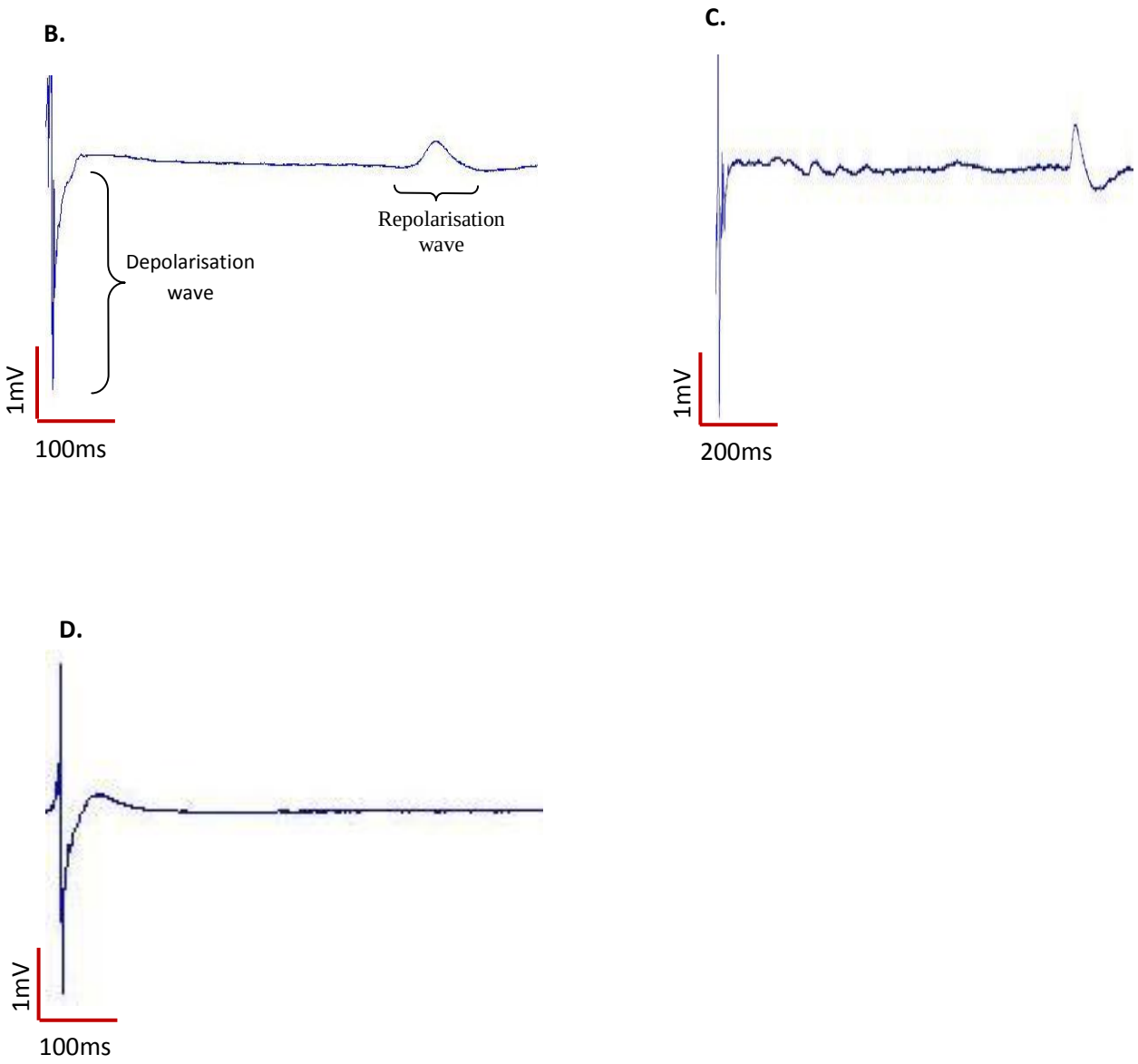

Figure 3: FP recordings. **A.** Overview of FPs of all 60 electrodes. Enlarged FPs waveform recordings showing detectable repolarisation wave in both dog and human (**B**, **C** respectively) which was undetectable in rat slices (**D**).

3.2.4 Effects of E-4031 on FPD

The FPD prolongation effect of 1μM E-4031, the I_{Kr} blocker, was not detectable in rat ventricular slices, whereas significantly prolonged FPD by 18% in dog ventricular slices, paced at 1 Hz. (Figure 4, 5)

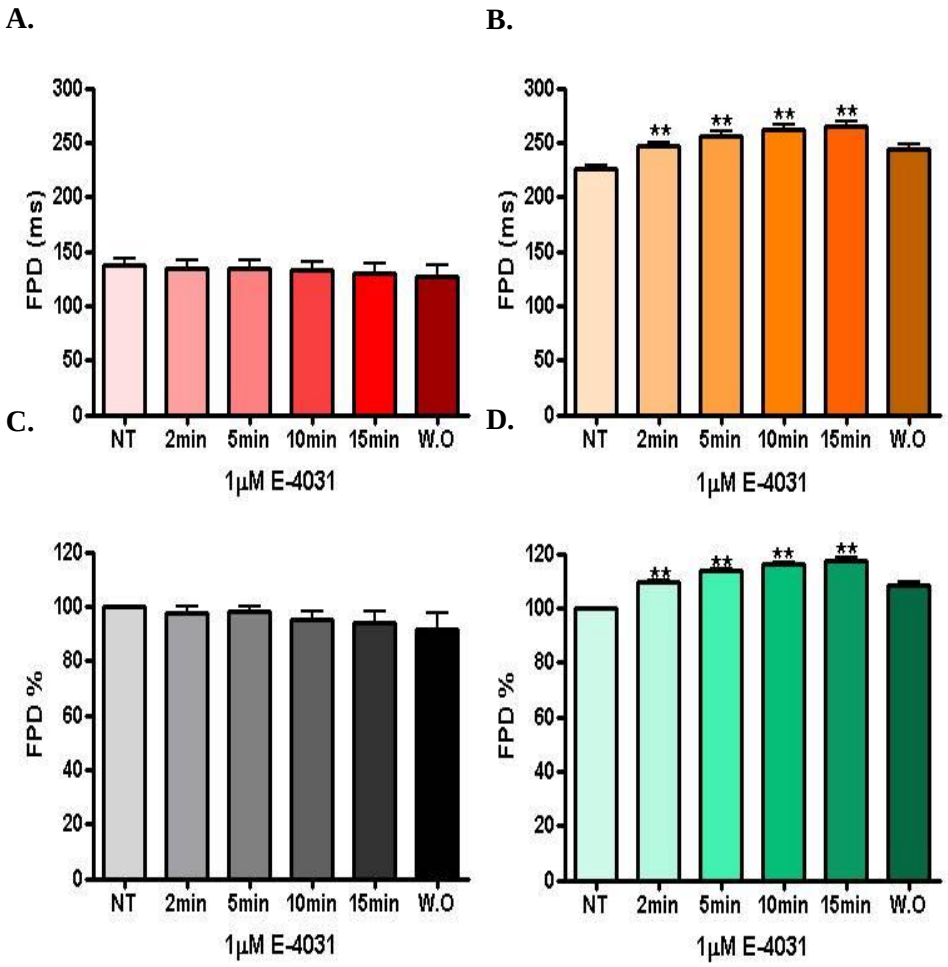

Figure 4: Effects of E-4031 on FPD in rat and dog ventricular slices. E-4031 shows non observable effect on FPD absolute values (ms) and relative values to control in rat ventricular myocardial slices (n= 4hearts/13slices, A and C). Prolongation effect by 18% was measured in dog ventricular slices (n= 6hearts/26slices, B and D). **P<0.001

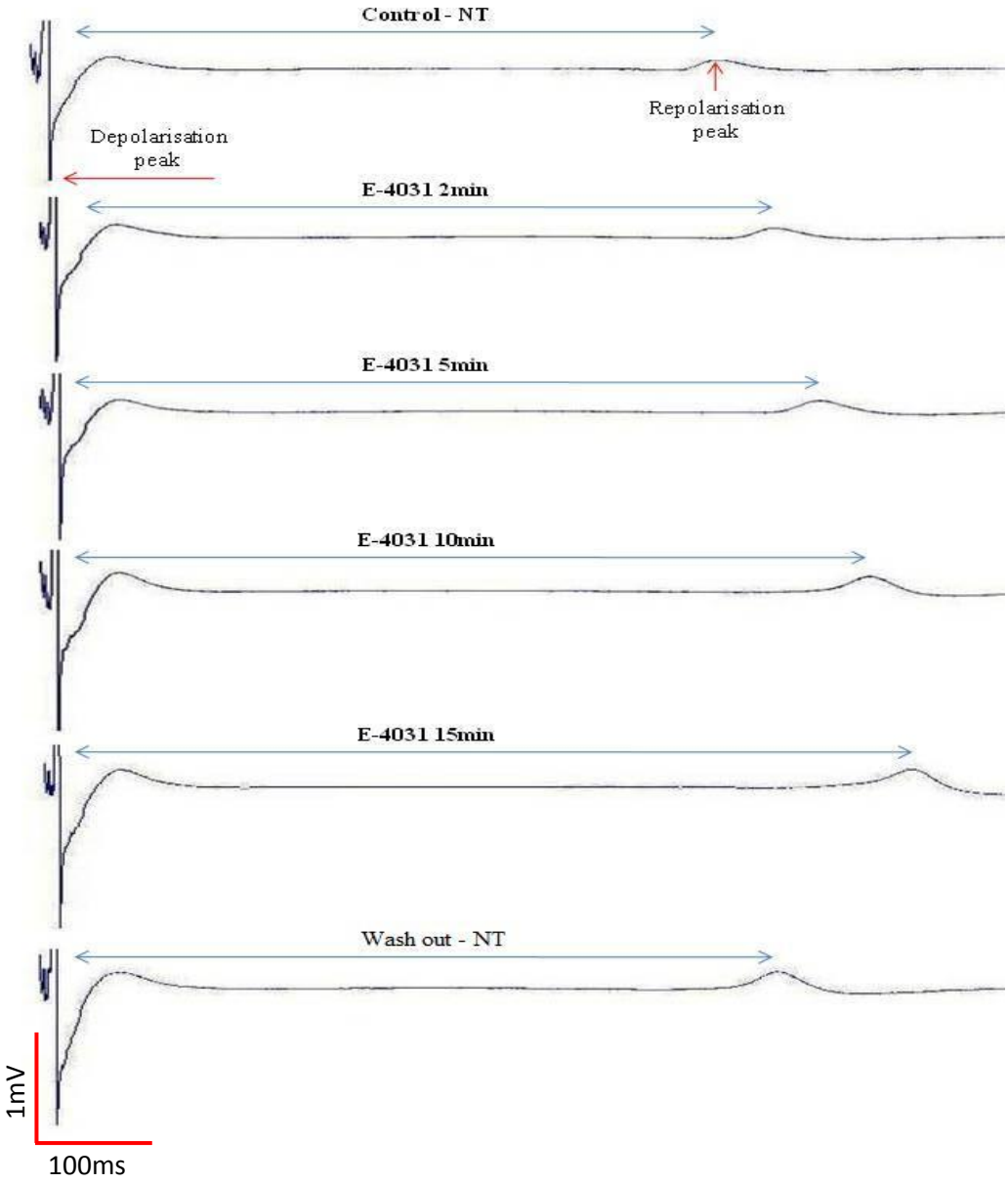

Figure 5: E-4031 shows prolongation of FPD in dog ventricular myocardial slices. Traces show FPD waveform before and after E-4031.

1μM E-4031 significantly prolonged FPD by 32% in human DCM slices and 29% in human myocarditis slices (stimulated at 1 Hz). (Figure 6)

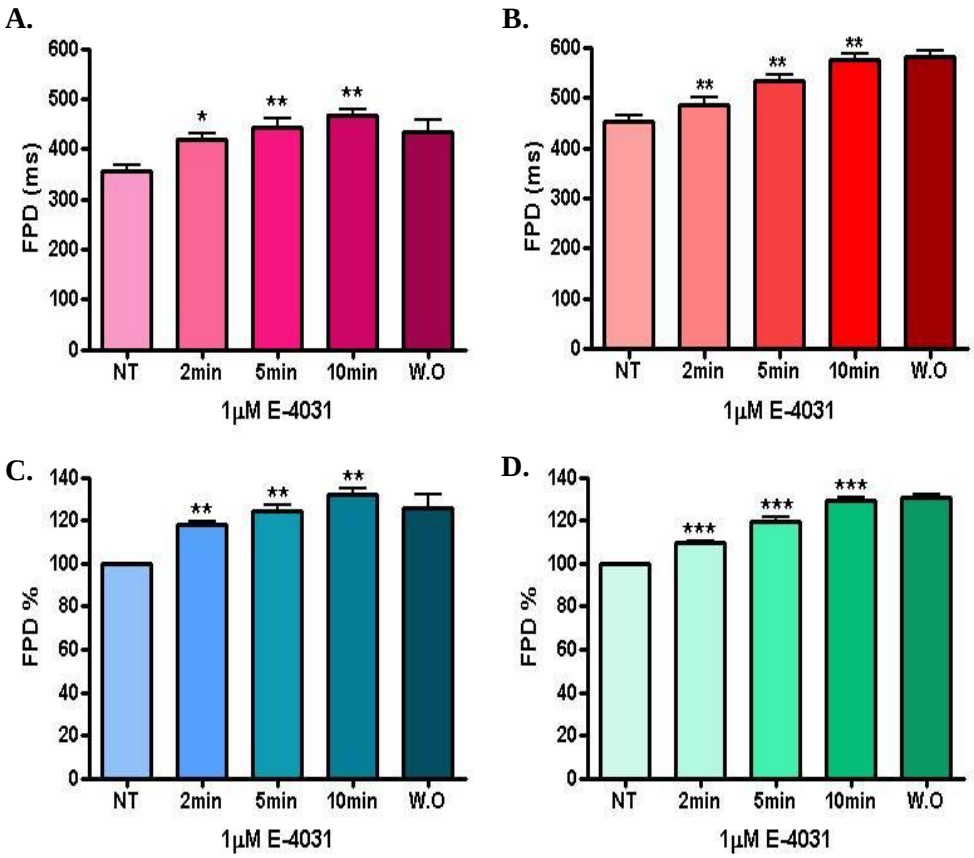

Figure 6: Effects of E-4031 on FPD in human ventricular slices. E-4031 shows prolongation effect in human DCM slices (n= 1heart/6slices, A and C), and in human myocarditis slices (n= 1heart/4slices, B and D). *P<0.05, **P<0.01, ***P<0.001

3.2.5 Effects of Chromanol 239B on FPD

The application of the I_{ks} blockade 20µM Chromanol 293B prolonged FPD by 10% in dog ventricular myocardial slices paced at 1Hz. (Figure 7)

A.

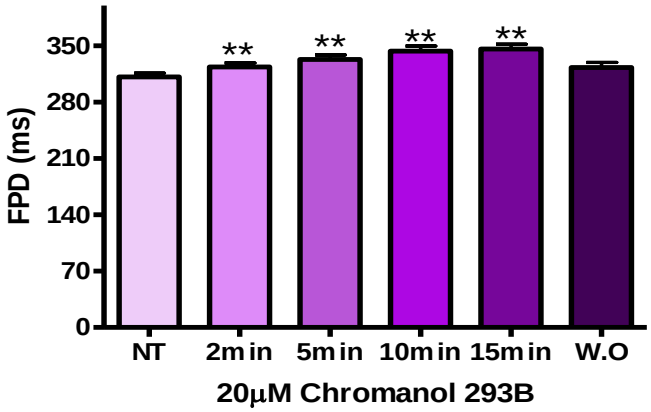

B.

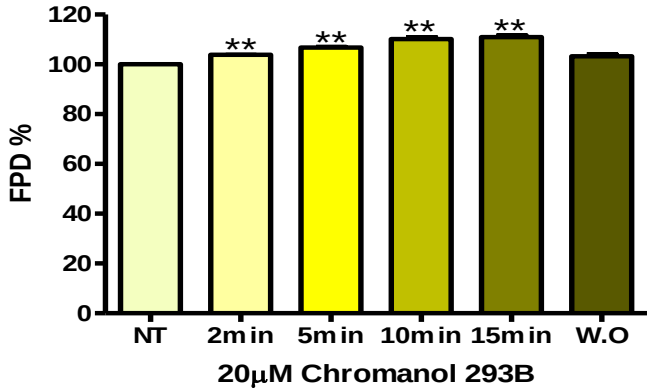

Figure 7: Effects of Chromanol 239B on FPD. Chromanol 293B shows prolongation effect in dog ventricular myocardial slices (n= 2hearts/9slices, **P<0.001).

3.3 CV Measurements

3.3.1 Effects of Different Superfusing Solutions on CV

In all our measurements NT solution has been used to superfused the cardiac slices. This was done for practical reasons as NT solution does not need continuous 5% CO_2 oxygenation, allowing the use of different superfusion lines and rapid switching between solutions. However, the lack of bicarbonate in the NT solution makes it less suitable for longer term experiments. To test whether this factor can affect the measurements obtained in this study, experiments were performed to compare the CV obtained using NT or KREBS solution. Rat Slices were superfused for 15 minutes. CVs measured showed no significant differences where CV was 31.82 ± 4.33 cm/s using NT and 39.17 ± 6.21 cm/s using KREBS. (Figure 8)

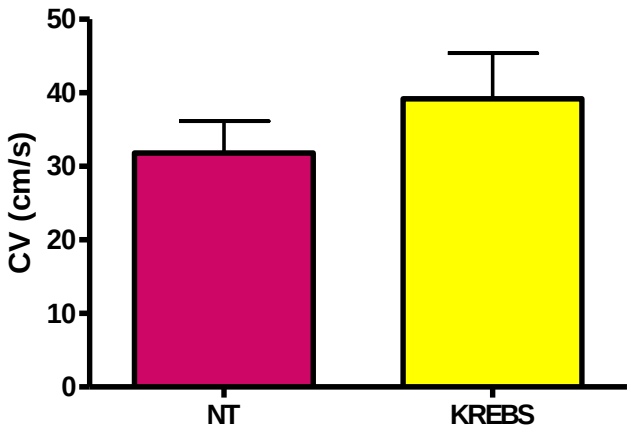

Figure 8: CV values measured for rat slices in the presence of NT or KREBS solution. No significant differences (P > 0.05) were detected.

3.3.2 Local and Peripheral CVs in Different Species

CV in slices was examined by measuring both local and peripheral velocities testing the slices uniform conduction patterns. Local velocity was calculated from each electrode to the neighbouring electrodes, while peripheral velocity was the mean conduction velocities measured from the extremities of the array (Meiry *et al.*, 2001) . Local - Peripheral findings were 32cm/s - 32 cm/s respectively in rat slices, 31cm/s - 37 cm/s in dog slices, 25cm/s - 34 cm/s in DCM slices, 25cm/s - 23cm/s in HCM slices and 31cm/s - 32 cm/s in myocarditis slices. (Figures 9, 10)

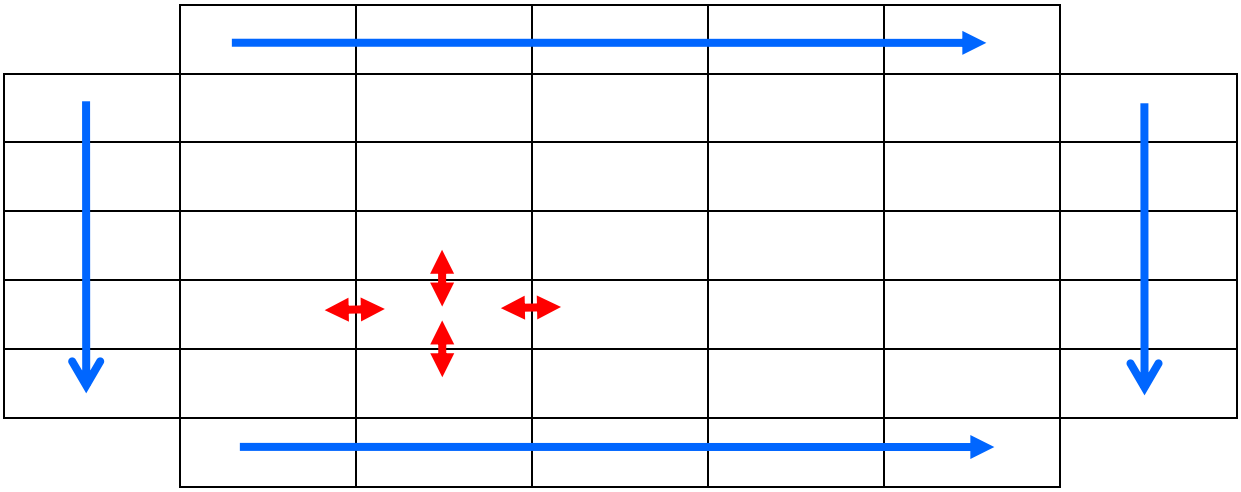

Figure 9: local and peripheral conduction velocities**.** Arrows represent how local (red), peripheral (blue) velocities were measured.

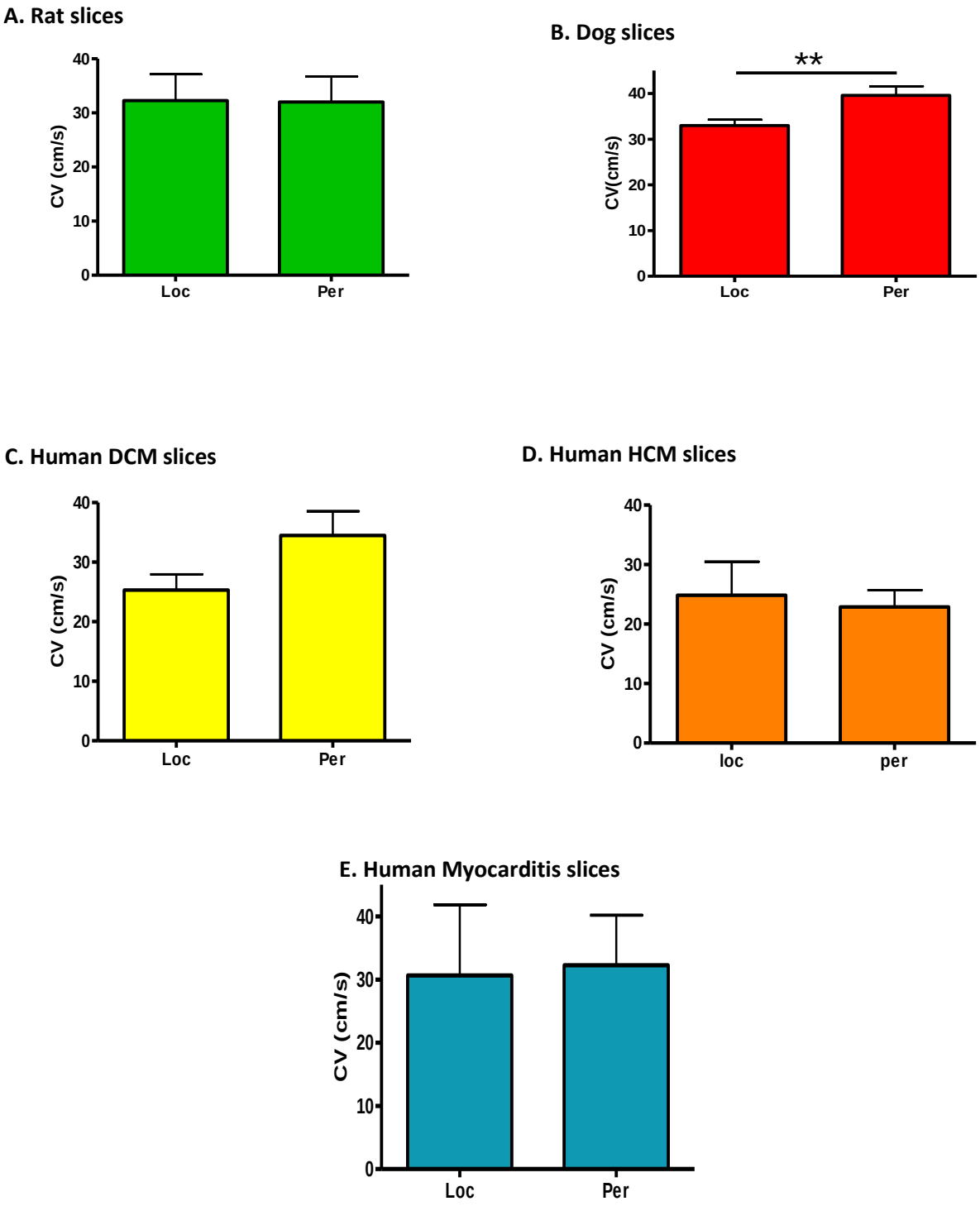

Figure 10: Local (Loc) and peripheral (Per) CVs measured in different species. **A.** Rat ventricular slices (n=4hearts/13slices, P=0.9). **B.** Dog ventricular slices (n=8hearts/39slices, **P=0.007). **C.** Human DCM slices (n=1heart/6slices, P=0.05). **D.** Human HCM slices (n=1heart/4slices, P=0.7). E. Human Myocarditis slices (n= 1heart/4slices, P=0.9)

3.3.3 Isochronal Map and Excitation Spread

Excitation spread was well demonstrated using isochronal maps. As an example, one of the dog slices was analysed depending on the fibres orientation (Figure11).

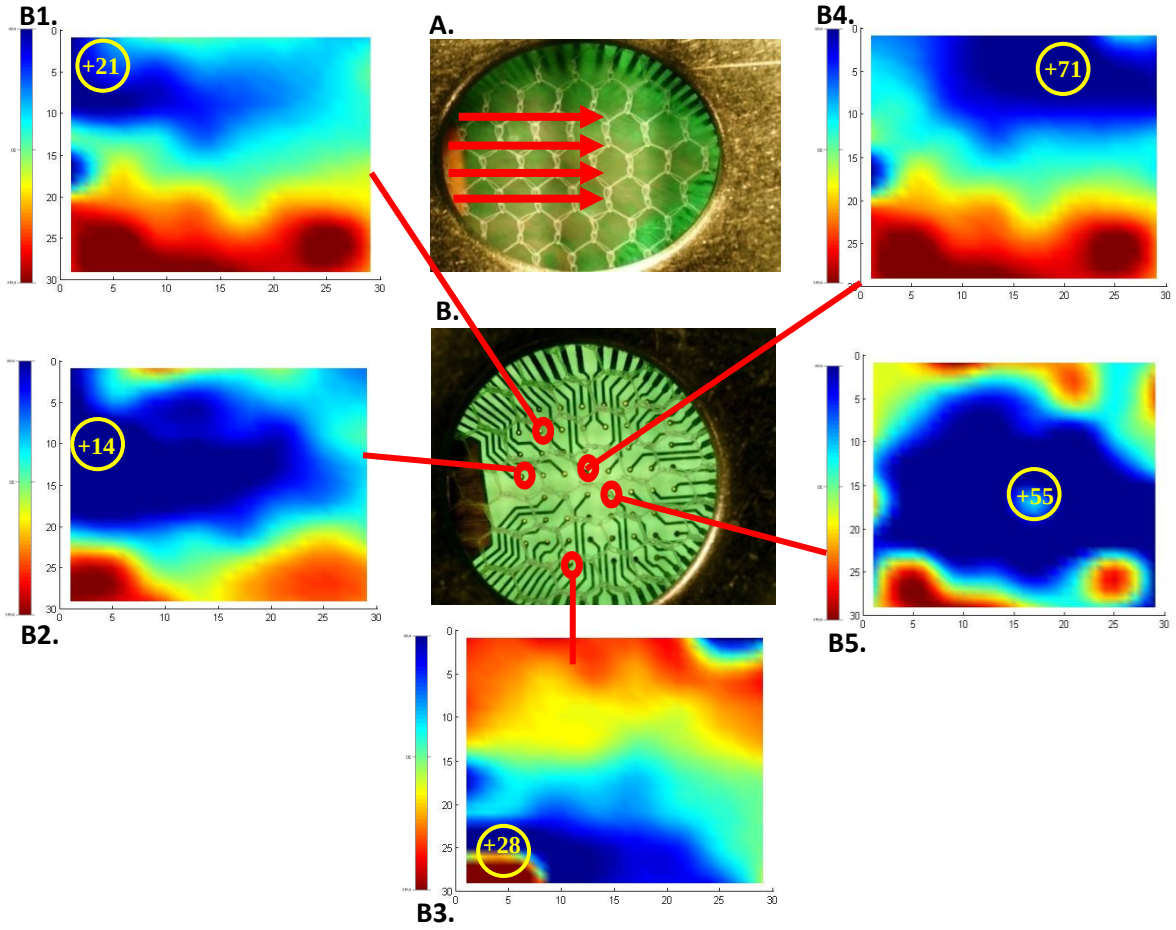

Figure 11: Two-dimensional spread of excitation in a dog ventricular myocardial slice. **A.** Dog cardiac slice in MEA dish (horizontal orientation of the fibres - red arrows). **B.** Overview of MEA dish with all 60 microelectrodes. Isochronal map showing the horizontal excitation spread after stimulating from different electrodes such as: electrode +21 **(B1),** electrode +14 (**B2**), electrode +28 (**B3**), electrode +71 (**B4),** and electrode +55 **(B5).**

3.3.4 Correlation between the Orientation of the Fibres & Different CVs

Anisotropic properties of the myocardial slices were tested while recording CV using different positions of the unipolar stimulating electrode. From obtained microscopic images, an assumption was made that the fastest electrical propagation would be obtained along the fibre direction, whilst the slowest would be in a perpendicular direction. Maximum velocity (MaxV) represents the velocity recorded within the same orientation whereas the Minimum velocity (MinV) represents the perpendicular orientation. MaxV/MinV results measured from different species were 61/28 (cm/s) from rat slices, 66/30 (cm/s) from dog, 55/17 (cm/s) from DCM slices, 39/14 (cm/s) HCM slices and 76/19 (cm/s) from Myocarditis slices. (Figure 12)

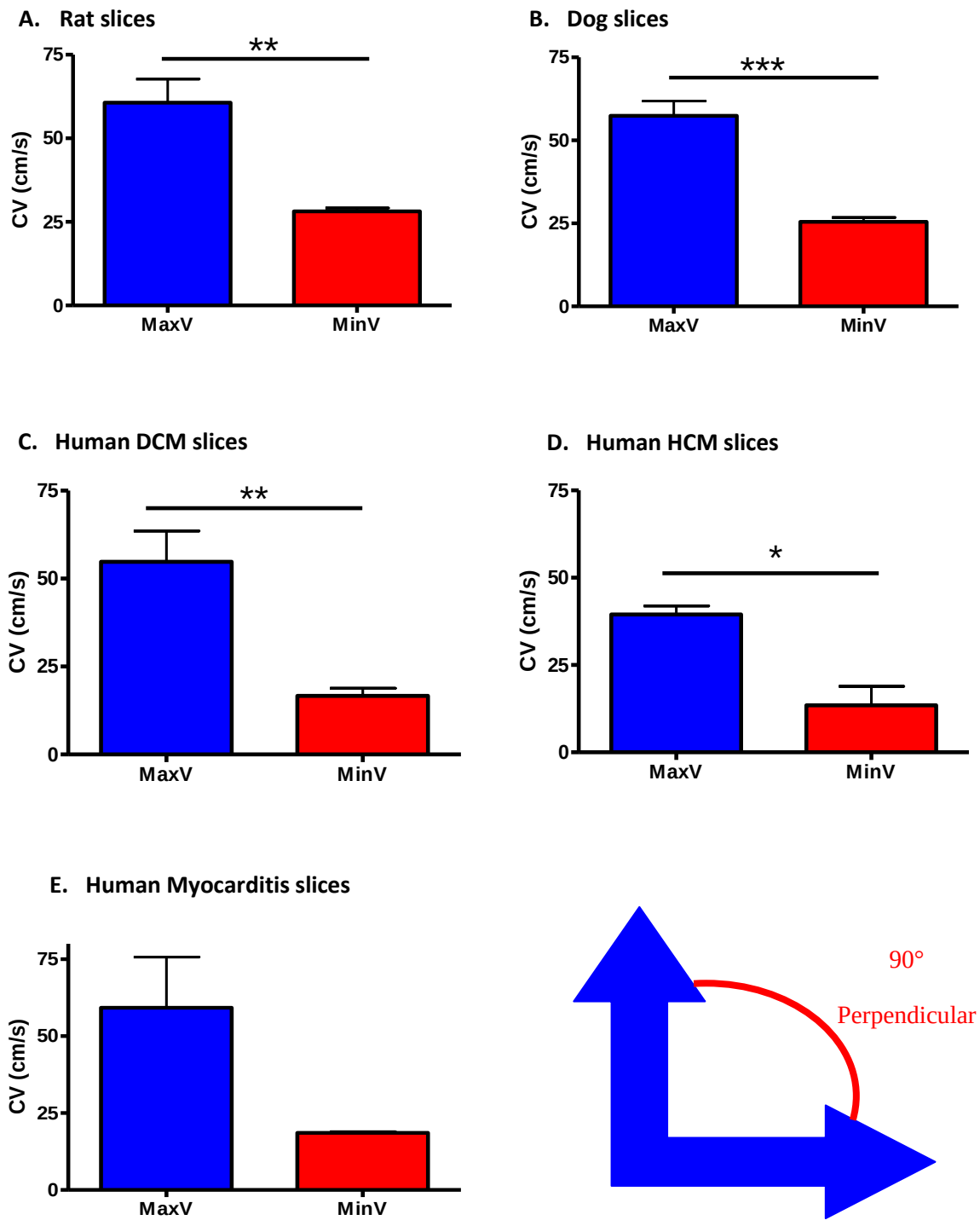

Figure 12: Anisotropic MaxV and MinV differences in different species. **A.** Rat ventricular slices (n=4hearts/12slices, **P=0.001). **B.** Dog ventricular slices (n=8hearts/29slices, ***P<0.0001). **C.** Human DCM slices (n=1heart/6slices, **P=0.0017). **D.** Human HCM slices (n=1heart/2slices, *P=0.049). **E.** Human Myocarditis slices (n=1heart/2slices, P=0.13).

4. DISCUSSION

4.1 Summary of the Main Results

This study has shown that ventricular slices are a representative tool for studying the electrophysiological pharmacological activities of the myocardium. The aims of my work were firstly to assess if the slices are viable for electrophysiological recordings using MEA and if the electrical recordings obtained from them mimic physiological readings, secondly to investigate pharmacological drugs effect, in addition to test cardiac tissue properties such as CV and anisotropism.

My first aim required a detailed characterisation of the slices electrophysiological function .For the second aim, I have tested the response of the slices to two well known delayed rectifier potassium channel blockers E4031 and Chromanol 293B.

The results show that slices have electrophysiological properties representative of native heart including APD_{90} and CV. In addition dog and human slices respond to the I_{Kr} or I_{ks} blockers with prolongation of FPD as already shown for APD_{90} in single cells.

4.2 Control FPs

Adult dog ventricular myocardial slices had FPD of 311.5 ± 4.97 ms. A study performed by Akar & Rosenbaum showed similar values: APD_{90} recorded from dog wedge preparation was 331 ± 16 ms (42).

This study showed that FPD in human DCM slices was 356.5 ± 10.72 ms and 452 ± 12.32 ms from Myocarditis slices, but due to the absence of normal heart tissue the comparison between the diseased and normal tissue slices was not possible. Previously obtained data showed that APD_{90} in human

papillary muscle or trabeculae from normal heart (obtained from healthy donors) was 320 ± 21 ms (14),443 ± 25 ms from DCM (14) and 351.1 ± 35.4 ms from papillary muscle slices (34). FPD was comparable between different cardiac preparations showing slight differences depending on the causal disease.

4.3 Pharmacological Investigations:

4.3.1 Effects of E-4031 in Different Species

E-4031 prolongs APD by blocking the rapid delayed rectifier potassium channel – I_{Kr} in cardiac tissue. Concentration of 1µM E-4031 was chosen due to the production of maximum response in guinea pig papillary muscle (14).

E-4031 prolongation was not detected in this study using rat ventricular tissue slices. However, E-4031 does not prolong the QT interval in isolated rat hearts (11). This is probably due to the lack of expression of I_{Kr} channels in rat ventricle tissue (43-45).

In normal dog cardiac tissues E-4031 prolonged FPD as expected. In dog myocardial slices 18% FPD prolongation was detected. In other study E-4031 has prolonged APD_{90} by 19% in the whole heart using epicardial mapping (46). Dog isolated cardiomyocytes, ventricular papillary muscle and purkinje fibre APD_{90} was prolonged markedly by 20% (12).

Application of E-4031 significantly prolonged APD in human cardiac tissue. Our experiments using E-4031 resulted in 32% prolongation in human DCM slices and 29% in human myocarditis slices. Others showed 26.5% in human papillary muscle slice and 47% in intact human papillary muscle (34), and 66% normal , 59% DCM human papillary muscle or trabeculae (14).

4.3.2 Effects of Chromanol 293B

FPD prolongation induced by Chromanol 293B is due to the inhibition of the slow delayed rectifier potassium channel (16). 10µM Chromanol 293B did not markedly lengthen APD in dog ventricular

isolated cardiomyocytes, papillary muscle and purkinje fibres showing less than 7% prolongation (12;17;47).

In this study, higher concentration of Chromanol 293B has been used. 20µM Chromanol 293B prolonged dog ventricular myocardial slices FPD by 10%. The resulted prolongation can be due to either a direct block of I_{ks} or the specific effect of the drug on I_{to} as previously reported (13;17).

4.4 Slices Homogeneity

Local and peripheral CVs similarities are an indication of slices homogeneity. This study showed (local CV– peripheral CV, respectively) 32cm/s - 32 cm/s in rat slices, 31cm/s - 37 cm/s in dog slices, 25cm/s – 23cm/s in HCM slices, 31 cm/s – 32 cm/s in myocarditis slices, and 25cm/s -34cm/s in DCM slices. Many factors might lead to dissimilarity of local and peripheral CVs such as discontinuity of muscle fibres due to fat infiltration, blood vessels penetration, and fibrotic tissue localization due to different pathologies in myocardial tissue slices and presence of injured cells in the slice peripheries.

4.5 Anisotropism

Due to higher resistance in transverse myocyte-to-myocyte connections, the AP propagation is slower in transverse axis than in longitudinal axis (22;23). CVs measured from the different species during longitudinal and transverse propagation are in agreement with measurements in the literature.

CV measurements obtained from rat myocardial slices were approximately 61 cm/s longitudinally and 28 cm/s transversally. In a study performed using, rat whole hearts showed similar values 61 cm/s longitudinally and transversally was 44 cm/s (48) .

Dog ventricular slices showed that longitudinal excitation speed is 2.4 times faster than transversal excitation speed measured from the whole heart (using multiterminal epicardial electrode)(22) showing 66 cm/s and 27 cm/s longitudinal and transverse velocities, respectively.

Diseased human myocardial slices tested here showed a CV of 17 cm/s MinV and 55 cm/s MaxV in human DCM slices, 40 cm/s MaxV and 13 cm/s MinV obtained from HCM myocardial slices, and from myocarditis tissue 59 cm/s and 19 cm/s . Human normal heart conduction velocities recorded by others were 41 cm/s as minimum and 87 cm/s as maximum (49). Diseased myocardial slices showed slower conduction velocities than normal. Because of the myocardial disarray, which is abnormal alignment of myocytes that can be seen in HCM patient, CV was the slowest (50).

4.6 Study Limitation

As any other model, there were several limitations in the use of myocardial slices. These include the absence of the haemodynamic and neurohormonal control, ventricular wall pressure and normal tissue stretching (tension). For the anisotropic measurements, the excitation propagation was measured according to the fibres orientation which was either longitudinally or transversely but in normal beating heart the propagation is not purely in either direction. For human heart investigations, lack of control tissue and minimum numbers of cardiac surgeries were the main limitations.

4.7 Future Direction

Viable slices are suitable for a variety of investigations such as pharmacological testing using cardiac and non-cardiac drugs and conduction velocity measurements in regard to the aging process and the distribution of gap junctions.

4.8 Conclusion

Reproducible and viable living adult myocardial tissue slices can be prepared from different species such as rat, dog, and human. The slices are electrophysiologically intact, have physiological properties, and respond to different pharmacological tests in an expected manner.

Reference List

(1) Boyett MR. 'And the beat goes on.' The cardiac conduction system: the wiring system of the heart. Exp Physiol 2009 Oct;94(10):1035-49.

(2) Abramochkin DV, Sukhova GS, Rozenshtraukh LV. [Mechanisms of functioning and regulation of mammalian sinoatrial node]. Usp Fiziol Nauk 2009 Oct;40(4):21-41.

(3) Bers DM. Cardiac action potentials and ion channels. Excitation-Contraction Coupling and Cardiac Contractile Force. Second ed. Springer; 2002. p. 63-100.

(4) Marieb EN. Cells and Tissues. Essentials of Human Anatomy & Physiology. Seventh Edition ed. Daryl Fox; 2003. p. 56-94.

(5) Grant AO. Cardiac ion channels. Circ Arrhythm Electrophysiol 2009 Apr;2(2):185-94.

(6) Pongs O. Ins and outs of cardiac voltage-gated potassium channels. Curr Opin Pharmacol 2009 Jun;9(3):311-5.

(7) Goldstein SA, Bayliss DA, Kim D, Lesage F, Plant LD, Rajan S. International Union of Pharmacology. LV. Nomenclature and molecular relationships of two-P potassium channels. Pharmacol Rev 2005 Dec;57(4):527-40.

(8) Hibino H, Inanobe A, Furutani K, Murakami S, Findlay I, Kurachi Y. Inwardly rectifying potassium channels: their structure, function, and physiological roles. Physiol Rev 2010 Jan;90(1):291-366.

(9) Wulff H, Castle NA, Pardo LA. Voltage-gated potassium channels as therapeutic targets. Nat Rev Drug Discov 2009 Dec;8(12):982-1001.

(10) Sanguinetti MC, Tristani-Firouzi MT. Gating of Cardiac Delayed Rectifier Potassium Channels. Cardiac Electrophysiology-From Cell to Beside. Fifth Edition ed. Saunders Elsevier; 2009. p. 105-13.

(11) Shinmura K, Tani M, Hasegawa H, Ebihara Y, Nakamura Y. Effect of E4031, a class III antiarrhythmic drug, on ischemia- and reperfusion-induced arrhythmias in isolated rat hearts. Jpn Heart J 1998 Mar;39(2):183-97.

(12) Varro A, Balati B, Iost N, Takacs J, Virag L, Lathrop DA, et al. The role of the delayed rectifier component IKs in dog ventricular muscle and Purkinje fibre repolarization. J Physiol 2000 Feb 15;523 Pt 1:67-81.

(13) Bosch RF, Gaspo R, Busch AE, Lang HJ, Li GR, Nattel S. Effects of the chromanol 293B, a selective blocker of the slow, component of the delayed rectifier K+ current, on repolarization in human and guinea pig ventricular myocytes. Cardiovasc Res 1998 May;38(2):441-50.

(14) Ohler A, Ravens U. Effects of E-4031, almokalant and tedisamil on postrest action potential duration of human papillary muscles. J Pharmacol Exp Ther 1994 Aug;270(2):460-5.

(15) Sanguinetti MC, Jurkiewicz NK. Two components of cardiac delayed rectifier K+ current. Differential sensitivity to block by class III antiarrhythmic agents. J Gen Physiol 1990 Jul;96(1):195-215.

(16) Suessbrich H, Bleich M, Ecke D, Rizzo M, Waldegger S, Lang F, et al. Specific blockade of slowly activating I(sK) channels by chromanols -- impact on the role of I(sK) channels in epithelia. FEBS Lett 1996 Nov 4;396(2-3):271-5.

(17) Sun ZQ, Thomas GP, Antzelevitch C. Chromanol 293B inhibits slowly activating delayed rectifier and transient outward currents in canine left ventricular myocytes. J Cardiovasc Electrophysiol 2001 Apr;12(4):472-8.

(18) Bernstein SA, Morley GE. Gap junctions and propagation of the cardiac action potential. Adv Cardiol 2006;42:71-85.

(19) Kanno S, Saffitz JE. The role of myocardial gap junctions in electrical conduction and arrhythmogenesis. Cardiovasc Pathol 2001 Jul;10(4):169-77.

(20) Uzzaman M, Honjo H, Takagishi Y, Emdad L, Magee AI, Severs NJ, et al. Remodeling of gap junctional coupling in hypertrophied right ventricles of rats with monocrotaline-induced pulmonary hypertension. Circ Res 2000 Apr 28;86(8):871-8.

(21) Emdad L, Uzzaman M, Takagishi Y, Honjo H, Uchida T, Severs NJ, et al. Gap junction remodeling in hypertrophied left ventricles of aortic-banded rats: prevention by angiotensin II type 1 receptor blockade. J Mol Cell Cardiol 2001 Feb;33(2):219-31.

(22) Roberts DE, Hersh LT, Scher AM. Influence of cardiac fiber orientation on wavefront voltage, conduction velocity, and tissue resistivity in the dog. Circ Res 1979 May;44(5):701-12.

(23) Valderrabano M. Influence of anisotropic conduction properties in the propagation of the cardiac action potential. Prog Biophys Mol Biol 2007 May;94(1-2):144-68.

(24) Koura T, Hara M, Takeuchi S, Ota K, Okada Y, Miyoshi S, et al. Anisotropic conduction properties in canine atria analyzed by high-resolution optical mapping: preferential direction of conduction block changes from longitudinal to transverse with increasing age. Circulation 2002 Apr 30;105(17):2092-8.

(25) Wexler RK, Elton T, Pleister A, Feldman D. Cardiomyopathy: an overview. Am Fam Physician 2009 May 1;79(9):778-84.

(26) Luk A, Ahn E, Soor GS, Butany J. Dilated cardiomyopathy: a review. J Clin Pathol 2009 Mar;62(3):219-25.

(27) Yoerger DM, Weyman AE. Hypertrophic obstructive cardiomyopathy: mechanism of obstruction and response to therapy. Rev Cardiovasc Med 2003;4(4):199-215.

(28) Blauwet LA, Cooper LT. Myocarditis. Prog Cardiovasc Dis 2010 Jan;52(4):274-88.

(29) Boilson BA, Raichlin E, Park SJ, Kushwaha SS. Device therapy and cardiac transplantation for end-stage heart failure. Curr Probl Cardiol 2010 Jan;35(1):8-64.

(30) Schrickel JW, Kreuzberg MM, Ghanem A, Kim JS, Linhart M, Andrie R, et al. Normal impulse propagation in the atrioventricular conduction system of Cx30.2/Cx40 double deficient mice. J Mol Cell Cardiol 2009 May;46(5):644-52.

(31) de Boer TP, Camelliti P, Ravens U, Kohl P. Myocardial tissue slices: organotypic pseudo-2D models for cardiac research & development. Future Cardiol 2009 Sep;5(5):425-30.

(32) Pillekamp F, Halbach M, Reppel M, Rubenchyk O, Pfannkuche K, Xi JY, et al. Neonatal murine heart slices. A robust model to study ventricular isometric contractions. Cell Physiol Biochem 2007;20(6):837-46.

(33) Halbach M, Pillekamp F, Brockmeier K, Hescheler J, Muller-Ehmsen J, Reppel M. Ventricular slices of adult mouse hearts--a new multicellular in vitro model for electrophysiological studies. Cell Physiol Biochem 2006;18(1-3):1-8.

(34) Bussek A, Wettwer E, Christ T, Lohmann H, Camelliti P, Ravens U. Tissue slices from adult mammalian hearts as a model for pharmacological drug testing. Cell Physiol Biochem 2009;24(5-6):527-36.

(35) Parrish AR, Gandolfi AJ, Brendel K. Precision-cut tissue slices: applications in pharmacology and toxicology. Life Sci 1995;57(21):1887-901.

(36) Neri B, Cini-Neri G, D'Alterio M. Effect of anthracyclines and mitoxantrone on oxygen uptake and ATP intracellular concentration in rat heart slices. Biochem Biophys Res Commun 1984 Dec 28;125(3):954-60.

(37) Yamashita D, Kohzuki H, Kitagawa Y, Nakashima T, Kikuta A, Takaki M. O2 consumption of mechanically unloaded contractions of mouse left ventricular myocardial slices. Am J Physiol Heart Circ Physiol 2004 Jul;287(1):H54-H62.

(38) Burnashev NA, Edwards FA, Verkhratsky AN. Patch-clamp recordings on rat cardiac muscle slices. Pflugers Arch 1990 Sep;417(1):123-5.

(39) Camelliti P, Picton GK, Bub G, Bussek A, Wettwer E, Ravens U & Kohl P. Ventricular tissue slices as representative 3D models of myocardium. 2008.

(40) Dizon JM. Brugada Syndrome: Multimedia. emedicine from WebMD 2009 August 24 [cited 10 A.D. Jul 3];

(41) Halbach M, Egert U, Hescheler J, Banach K. Estimation of action potential changes from field potential recordings in multicellular mouse cardiac myocyte cultures. Cell Physiol Biochem 2003;13(5):271-84.

(42) Akar FG, Rosenbaum DS. Transmural electrophysiological heterogeneities underlying arrhythmogenesis in heart failure. Circ Res 2003 Oct 3;93(7):638-45.

(43) Pond AL, Scheve BK, Benedict AT, Petrecca K, Van Wagoner DR, Shrier A, et al. Expression of distinct ERG proteins in rat, mouse, and human heart. Relation to functional I(Kr) channels. J Biol Chem 2000 Feb 25;275(8):5997-6006.

(44) Pond AL, Nerbonne JM. ERG Proteins and Functional Cardiac IKr Channels in Rat, Mouse, and Human Heart. Trends in Cardiovascular Medicine 2001 Oct;11(7):286-94.

(45) Wymore RS, Gintant GA, Wymore RT, Dixon JE, McKinnon D, Cohen IS. Tissue and species distribution of mRNA for the IKr-like K+ channel, erg. Circ Res 1997 Feb;80(2):261-8.

(46) Ogawa S, Mitamura H, Katoh H. Effect of E-4031, a new class III antiarrhythmic drug, on reentrant ventricular arrhythmias: comparison with conventional class I drugs. Cardiovasc Drugs Ther 1993 Aug;7 Suppl 3:621-6.

(47) Abi-Gerges N, Small BG, Lawrence CL, Hammond TG, Valentin JP, Pollard CE. Gender differences in the slow delayed (IKs) but not in inward (IK1) rectifier K+ currents of canine Purkinje fibre cardiac action potential: key roles for IKs, beta-adrenoceptor stimulation, pacing rate and gender. Br J Pharmacol 2006 Mar;147(6):653-60.

(48) Mills WR, Mal N, Forudi F, Popovic ZB, Penn MS, Laurita KR. Optical mapping of late myocardial infarction in rats. Am J Physiol Heart Circ Physiol 2006 Mar;290(3):H1298-H1306.

(49) Nanthakumar K, Jalife J, Masse S, Downar E, Pop M, Asta J, et al. Optical mapping of Langendorff-perfused human hearts: establishing a model for the study of ventricular fibrillation in humans. Am J Physiol Heart Circ Physiol 2007 Jul;293(1):H875-H880.

(50) Nishihara K, Mikami T, Takatsuji H, Onozuka H, Saito N, Yamada S, et al. Usefulness of early diastolic flow propagation velocity measured by color M-mode Doppler technique for the assessment of left ventricular diastolic function in patients with hypertrophic cardiomyopathy. J Am Soc Echocardiogr 2000 Sep;13(9):801-8.